

Cross-Problem Solving for Network Optimization: Is Problem-Aware Learning the Key?

Ruihuai Liang, *Student Member, IEEE*, Bo Yang, *Member, IEEE*, Pengyu Chen, Xuelin Cao, *Member, IEEE*, Zhiwen Yu, *Senior Member, IEEE*, H. Vincent Poor, *Life Fellow, IEEE*, and Chau Yuen, *Fellow, IEEE*

Abstract—As intelligent network services continue to diversify, ensuring efficient and adaptive resource allocation in edge networks has become increasingly critical. Yet the wide functional variations across services often give rise to new and unforeseen optimization problems, rendering traditional manual modeling and solver design both time-consuming and inflexible. This limitation reveals a key gap between current methods and human solving — the inability to recognize and understand problem characteristics. It raises the question of whether problem-aware learning can bridge this gap and support effective cross-problem generalization. To answer this question, we propose a problem-aware diffusion (PAD) model, which leverages a problem-aware learning framework to enable cross-problem generalization. By explicitly encoding the mathematical formulations of optimization problems into token-level embeddings, PAD empowers the model to understand and adapt to problem structures. Extensive experiments across six diverse network optimization problems show that PAD generalizes well to unseen problems while significantly improving solution quality and feasibility. Meanwhile, an auxiliary constraint-aware module is designed to enforce solution validity further. The experiments reveal that problem-aware learning is promising for building general-purpose solvers for intelligent network operation and resource management. Our code is open source at <https://github.com/qiyu3816/PAD>.

Index Terms—Network optimization, resource allocation, problem-aware learning, generative diffusion model.

I. INTRODUCTION

THE vision of future wireless communication systems has been widely built in both academia and industry [1]–[5], with fundamental AI models capable of general problem-solving being pursued as a revolutionary technology. These intelligent fundamental AI models are expected to enable autonomous and general network operations across various tasks, such as network resource management [6] and data analysis [7]. Notably, the continuous emergence of novel intelligent services in wireless networks is driving an unprecedented demand for efficient allocation of network resources like power and spectrum. In future wireless networks, different types of

tasks—such as power allocation and spectrum allocation—will coexist within edge networks, while edge networks themselves may differ significantly in functionality and environmental settings (e.g., computation offloading networks and edge sensing networks), which inherently raises diverse network optimization problems with varying objectives, constraints, and mathematical formulations [5], [8]–[11]. However, most existing network optimization approaches treat each problem in isolation, failing to address them in a unified and seamless manner. Consequently, cross-problem network optimization is a key capability for the intelligent fundamental models of next-generation wireless communication systems.

Cross-problem network optimization presents several challenges with existing approaches. First, most methods [6], [12]–[16] rely on manually analyzing predefined problems and designing corresponding algorithms or models. This approach is labor-intensive thus impractical for achieving cross-problem generalization at scale. Additionally, AI philosophies theoretically capable of general-purpose problem-solving [17] often require extensive customization of hyperparameters and algorithms in practice. For example, problem-specific value networks [18], [19] introduce inefficiencies that make them unsuitable for cross-problem network optimization. Finally, AI-based network optimization methods [14], [20], [21] have long been criticized for their inability to strictly enforce hard constraints. These methods often rely entirely on externally curated rules to satisfy constraints, limiting their applicability.

Overall, most existing network optimization approaches either depend on expert-driven designs, making them inefficient, or function as statistical black boxes, lacking problem awareness, as shown in Fig. 1. They fail to leverage the model itself to learn to recognize and understand problem characteristics (e.g., mathematical structures) for problem-solving, which is how humans approach cross-problem tasks.

In this context, a key question raised: *Can problem-aware learning enable models to develop a meaningful understanding of problem objectives and achieve cross-problem generalization?* Inspired by recent advances in using large language models (LLMs) for mathematical reasoning [22], math question similarity calculation [23], and optimization problem modeling [24], we argue that the mathematical formulations of network optimization problems also contain instructive information that can help models better understand problem characteristics. Incorporating these representations into the model’s inference process can enhance the capacity for cross-problem solving. To address the aforementioned challenges, we propose a problem-aware diffusion (PAD) model designed

R. Liang, B. Yang and P. Chen are with the School of Computer Science, Northwestern Polytechnical University, Xi’an, Shaanxi, 710129, China (email: liangruihuai_npu, cpy_npu@mail.nwpu.edu.cn, yang_bo@nwpu.edu.cn).

Z. Yu is with the School of Computer Science, Northwestern Polytechnical University, Xi’an, Shaanxi, 710129, China, and Harbin Engineering University, Harbin, Heilongjiang, 150001, China (email: zhiwenyu@nwpu.edu.cn).

X. Cao is with the School of Cyber Engineering, Xidian University, Xi’an, Shaanxi, 710071, China (email: caoxuelin@xidian.edu.cn).

H. V. Poor is with the Department of Electrical and Computer Engineering, Princeton University, Princeton, NJ 08544, USA (email: poor@princeton.edu).

C. Yuen is with the School of Electrical and Electronics Engineering, Nanyang Technological University, Singapore (email: chau.yuen@ntu.edu.sg).

for cross-problem solution generation in network optimization within a single fundamental model. PAD explores a novel problem-aware approach that integrates the rich mathematical representations of optimization problems into model learning. To achieve this, PAD leverages feature embeddings of network optimization problem formulations from existing mathematical LLMs during both training and solution generation.

Specifically, we extract the most informative features from the raw token embeddings of MathBERT [25] or DeepSeek-Math [26] using a pooling mechanism based on token similarity scores. PAD adopts the latent diffusion model (LDM) [27] with a Transformer-based backbone [28], embedding both input parameters and optimization solutions into a latent space through a pre-trained encoder-decoder architecture. By conditioning the denoising process on both the embedded input parameters and the pooled problem representations, PAD enables explicit recognition and learning of mathematical structures, granting it a degree of generalization to entirely unseen optimization problems. To further enhance constraint satisfaction in the generated solutions, PAD introduces a constraint-aware module, which is used only during training. This module approximates the original constraints as complex non-linear functions and introduces a differentiable constraint loss into the PAD’s objective. It takes the problem representations, input parameters, and current solution as input, and outputs a binary classification signal (0-1) indicating constraint satisfaction. By integrating this validation loss, PAD strengthens adherence to hard constraints in network optimization, improving solution feasibility and quality across diverse problem settings.

Our main contributions lie in providing exploratory answers to the following questions:

- **Can problem-aware learning enhance cross-problem generalization in network optimization?** We propose PAD that achieves problem-aware generalization within a single foundational model. By incorporating mathematical feature embeddings of optimization problems, PAD demonstrates the value of learning the mathematical structures of network optimization problems, offering a novel approach for models to grasp problem characteristics and achieve cross-problem solving.
- **Can a constraint-aware module improve the feasibility of generated solutions?** PAD introduces a constraint-aware module, which significantly improves constraint satisfaction by incorporating a constraint loss during training. This provides an efficient mechanism for ensuring that the model’s outputs comply with the hard constraints of the original optimization problems.
- **How can raw problem-specific feature embeddings be effectively utilized in problem-aware learning?** To effectively extract key information from the token sequence of the raw problem embedding, we design a ranked pooling mechanism based on intra-sequence token similarity scores. This approach not only reduces sequence length and removes irrelevant information, but also remains highly sensitive to subtle changes in problem semantics. Empirically, our method outperforms other standard pooling techniques.

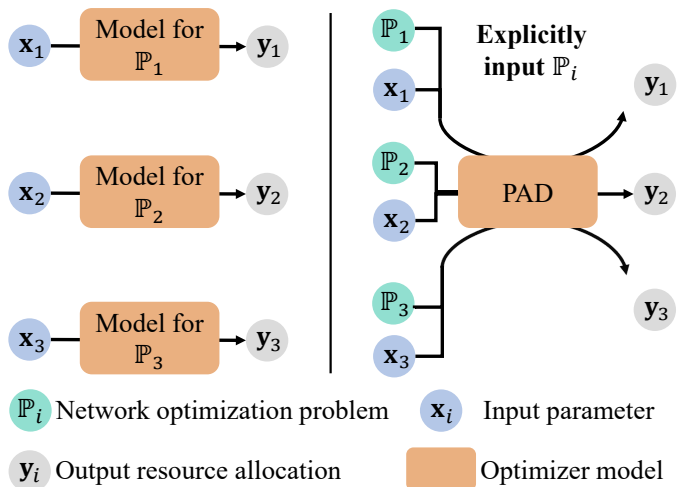


Fig. 1: Comparison of PAD with other isolated methods for cross-problem network optimization. PAD trains once and adapts to new problems via explicitly input \mathbb{P}_i , while traditional methods require re-training, even re-designing, for each individual problem.

II. PRELIMINARIES

A. Solution Generation for Network Optimization

Solution generation methods based on LLMs [9], [29], [30] and generative diffusion models (GDMs) [6], [21], [31]–[33] have achieved remarkable success in network optimization tasks. These approaches leverage the strong logical reasoning capabilities of LLMs and the powerful solution distribution modeling of diffusion models to produce superior solutions for specific problems. As data-driven approaches, generative models differ fundamentally from discriminative models. While discriminative models learn conditional probability distributions, generative models learn joint distributions, which makes their inference process inherently a form of sampling rather than classification or regression. This sampling-based inference allows for parallel generation and offers a more global understanding of the task compared to the fixed-output nature of common regression models. Generative AI (GenAI)-based frameworks for network management and optimization are rapidly gaining momentum in the communication network community. With their strong scaling laws, GenAI is increasingly seen as a promising candidate for serving as a foundational model in future communication systems.

B. Cross-Problem Solving

Existing approaches have explored cross-problem generalization from various perspectives. [34] analyzes the feasibility of joint training on different optimization problems within a single model by computing the cosine similarity between their gradient descent directions. [35] enhances cross-problem and cross-scale solution generation by conditioning a pre-trained model on energy-guided scores derived from problems similar to the original one. Meanwhile, [29] and [18] adopt LLMs and GDMs, respectively, as actors, leveraging deep reinforcement

learning (DRL) paradigms for cross-problem solving. However, these methods often rely on prior knowledge such as the optimal solution score [35] or a fixed problem space [29], or require building additional modules from scratch for each new task [18], [34]. In practical network optimization scenarios, neither the optimal objective score nor the full scope of new problems is typically available, and retraining models from scratch for every new case is infeasible.

C. Problem-Aware Learning

Problem-aware learning refers to a class of learning methods being explicitly informed or guided by the structure, objectives, or constraints of the underlying problem being solved, instead of learning patterns purely from data in a black-box way [36]. For example, [37] employs LLMs to iteratively generate solutions for simple optimization problems based on natural language descriptions, and [30] leverages domain-specific LLMs to produce resource allocation solutions for network optimization problems described in natural language. In addition, [38] advocates integrating formal methods (such as mathematical algorithms or rules) with machine learning, similar to problem-aware learning. However, [38] is limited to combining simple constrained problems into losses in the form of Lagrange functions, and is challenging to apply to network optimization problems where non-differentiable functions are standard.

Other related works explicitly leverage mathematical expressions to enhance the capabilities of LLMs on various tasks. In [24], the domain-specific LLM “TelecomGPT” is used to generate mathematical formulations from natural language descriptions. These generated formulations are then compared with ground truth using MathBERT and cosine similarity, demonstrating that LLMs can extract meaningful representations from network optimization problems. In the AI for Math community [22], [23], reasoning based on mathematical descriptions and problem formulations has been deeply investigated. Compared to relying on optimal solution scores or predefined problem spaces, acquiring mathematical formulations of network optimization problems is more realistic and informative. It can substantially benefit the design of problem-aware learning.

However, the natural language process (NLP)-centric framework of LLMs lacks precision in solution generation, often requiring repeated iterations based on feedback, and their training and inference costs are disproportionately high relative to the task. Although capable of performing direct problem-aware learning, they are not suitable for real-time implementation in network optimization.

At the same time, the potential of GDMs for cross-problem generalization has been validated in the AI community [39], [40]. Nevertheless, these works primarily focus on control problems, which differ significantly from network optimization in both formulation and application. Therefore, we believe integrating GDMs with problem-aware learning is a promising direction toward achieving cross-problem solving for network optimization.

III. SYSTEM MODEL

A. Cross-Problem Network Optimization

Network optimization problems arise from the need to allocate limited resources, such as communication and computation capacity, among various tasks. The objective is to determine the optimal resource allocation strategy that maximizes service performance under resource constraints, which are typically formulated and solved as mathematical optimization problems [11]. These mathematical formulations usually have the following form

$$\mathbb{P} : \min_{\mathbf{y}} f(\mathbf{x}, \mathbf{y}), \text{ s.t. } g(\mathbf{x}, \mathbf{y}) > 0, \quad (1)$$

where M -dimensional vector $\mathbf{x} \in \mathbb{R}^M$ denotes the input parameters such as network states and task-related information, while N -dimensional vector $\mathbf{y} \in \mathbb{R}^N$ represents the optimization variables such as power allocation and spectrum assignment. The functions $f : \mathbb{R}^{M+N} \rightarrow \mathbb{R}$ and $g : \mathbb{R}^{M+N} \rightarrow \mathbb{R}$ correspond to the objective function and the constraint function, respectively.

Cross-problem network optimization refers to the ability of a method to generalize across structurally and semantically different optimization problems, while preserving solution quality and not requiring task-specific redesign. The problems in this set may differ in objective function structure, constraint form, and semantic interpretation of inputs and outputs. As illustrated in Fig. 1, different network optimization problems such as \mathbb{P}_1 and \mathbb{P}_2 may have distinct mathematical semantics in their objective functions f_1 and f_2 , as well as in their constraint functions g_1 and g_2 . They may also differ in their input parameters $\mathbf{x}_1, \mathbf{x}_2$ and output variables $\mathbf{y}_1, \mathbf{y}_2$.

Traditional isolated optimizers rely on intensive human effort while limiting their applicability to narrowly scoped scenarios. Cross-problem network optimization offers a promising path toward efficient, automated, and scalable network operations in increasingly dynamic environments. However, as described in Section II, these models do not explicitly incorporate the mathematical structure of the problems during training, resulting in limited adaptability to new tasks.

We aim to enhance cross-problem generalization by embedding problem-specific mathematical information into model training, enabling direct adaptation to previously unseen tasks. These problem feature embeddings can be efficiently extracted from existing math-domain LLMs, and their informativeness and mathematical value have already been well recognized and validated [22]–[24]. Although perfect generalization across all network optimization problems may not be achievable, our method aims to generalize over a broad problem space without requiring a fixed number of predefined tasks.

B. Selected Optimization Problems

In this section, we provide an overview of the set of network optimization problems considered in our implementation. The problem selection is based on three key principles: 1) the problems must involve the allocation of major network resources; 2) the problems should include diverse types of input features and optimization variables with different physical meanings;

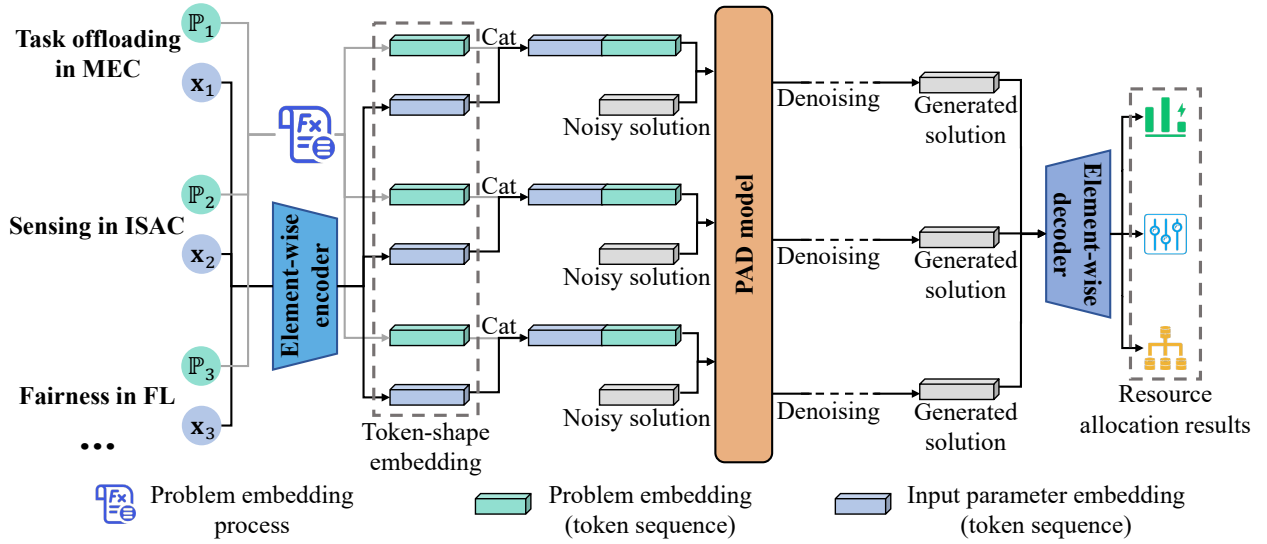


Fig. 2: Implementation framework of PAD.

3) the problems should cover a wide range of objectives and constraints to reflect the diversity of optimization problems encountered in real-world scenarios. Specifically, we consider six problems:

- 1) Power allocation aiming to maximize total transmission rate, subject to minimum rate constraints per link;
- 2) Power allocation aiming to maximize power efficiency, subject to minimum rate constraints per link;
- 3) Power allocation aiming to minimize the maximum transmission delay;
- 4) Spectrum resource block allocation aiming to maximize total transmission rate, subject to minimum rate constraints per link;
- 5) Spectrum resource block allocation aiming to maximize spectral efficiency, subject to minimum rate constraints per link;
- 6) Spectrum resource block allocation aiming to maximize total transmission rate, subject to fairness constraints.

The detailed mathematical formulations of these problems are provided in the **Appendix**.

These problems include two fundamental resource types: power [30], [41], [42] and spectrum [31], [43], [44], which are among the most critical optimization variables in wireless networks. The selected problems involve both continuous (real-valued) and discrete (integer-valued) variables, reflecting the real-world diversity of decision spaces. Standard parameters such as channel gains, data volumes, and noise power are incorporated to enhance the realism further. The objectives and constraints of these problems are inspired by key application scenarios, including multi-access edge computing (MEC) networks [45], integrated sensing and communication (ISAC) networks [3], and federated learning (FL) systems [46]. The problems cover various optimization types, from classical convex optimization to more challenging non-convex optimization and integer programming. By evaluating the proposed PAD across this selected and diverse problem set, we aim to demonstrate its effectiveness in handling different optimization structures and generalizing across diverse tasks.

IV. METHODOLOGY

A. Basics

To enable problem-aware learning, we first illustrate the theoretical advantages of incorporating mathematical problem embedding into the model by analyzing its impact on the learning objective. Let the process of problem feature embedding be denoted as $\mathbf{e}_i = \text{PE}(f_i, g_i)$, where i represents the index of a problem instance in the problem set, and \mathbf{e}_i is the resulting embedding sequence. Without incorporating problem embeddings, the theoretical learning objective becomes

$$p(\mathbf{y}_i, \mathbf{e}_i | \mathbf{x}_i) = \frac{p(\mathbf{y}_i, \mathbf{e}_i, \mathbf{x}_i)}{p(\mathbf{x}_i)}, \quad (2)$$

where the model must learn a joint mapping from the input parameter \mathbf{x}_i to both the associated problem \mathbf{e}_i and its corresponding solution.

Similarly, the learning objective after incorporating problem embeddings becomes

$$p(\mathbf{y}_i | \mathbf{e}_i, \mathbf{x}_i) = \frac{p(\mathbf{y}_i, \mathbf{e}_i, \mathbf{x}_i)}{p(\mathbf{e}_i, \mathbf{x}_i)}, \quad (3)$$

In the context of network optimization, different problems may share the same network state parameters and resource allocation variables. As a result, the optimization variable \mathbf{y} and the input parameter \mathbf{x} are both conditionally independent of the problem embedding \mathbf{e} . Therefore, we have $p(\mathbf{e}_i, \mathbf{x}_i) = p(\mathbf{e}_i)p(\mathbf{x}_i)$, where $p(\mathbf{e}_i) < 1$, leading to

$$p(\mathbf{y}_i | \mathbf{e}_i, \mathbf{x}_i) > p(\mathbf{y}_i, \mathbf{e}_i | \mathbf{x}_i). \quad (4)$$

Intuitively, Eq. (4) implies that the learning objective in Eq. (3) is more deterministic and effective than that in Eq. (2).

Specifically, due to the independence between \mathbf{x} and \mathbf{e} , attempting to infer the problem embedding \mathbf{e}_i directly from \mathbf{x}_i in Eq. (2) is theoretically flawed and likely to introduce noise. Moreover, assuming the output space of \mathbf{y} is of size Y , and that of \mathbf{e} is E (even though both are infinite in practice), the output space of Eq. (2) becomes $Y \times E$, which is significantly larger than the output space Y of Eq. (3). This leads to a sparsity of

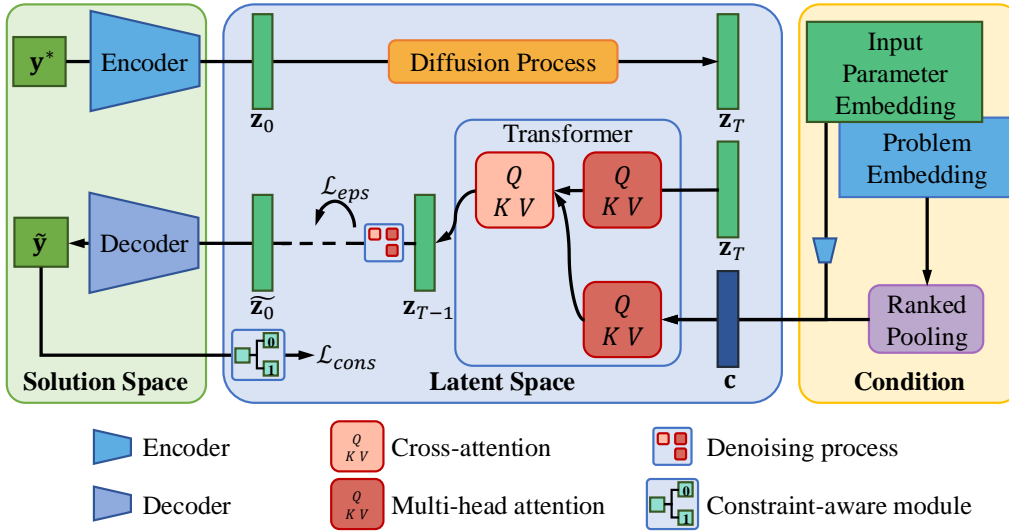


Fig. 3: Neural network structure of PAD.

training samples per output configuration in Eq. (2), making learning less efficient and more prone to underfitting.

In summary, by explicitly leveraging problem embeddings, Eq. (3) avoids the uncertainty and redundancy inherent in the joint modeling of problem and solution in Eq. (2). This brings a more focused learning objective with stronger generalization capability, making it a theoretically superior choice.

B. Ranked Pool for Problem Feature Embedding

The token sequence length of LLM-embedded mathematical formulations varies with the length of the underlying expressions. Although PAD leverages a Transformer-based architecture, such variable-length problem embeddings pose challenges for efficient learning. Hence, a token selection mechanism is required to extract key information into a fixed-length sequence. We observe that raw problem embeddings exhibit three distinct characteristics:

- 1) **Structural Sparsity.** Mathematical formulations of optimization problems are inherently structured, featuring segmented semantic components such as objective functions, constraints, and optimization variables. However, the corresponding tokens are often distributed sparsely and non-contiguously across the sequence, making retrieving meaningful structure more difficult.
- 2) **Symbol Sensitivity.** Small changes in mathematical symbols can lead to entirely different problem types. Moreover, global operators such as \min , \sum , or nested formulations require the structural integrity of the expression to be preserved during token selection.
- 3) **Long-Tail Distribution.** Standard low-level tokens (e.g., basic operators or variable names) appear frequently but carry limited semantic value. In contrast, high-information global symbols appear less often but are critical for understanding problem structure. A robust token selection mechanism must retain and emphasize these rare but informative tokens.

Conventional pooling strategies struggle to handle these properties. For instance, MaxPool [47], which selects the most

active tokens at each dimension, is highly susceptible to noise and often overemphasizes frequent but low-informative symbols (e.g., repeating input variable names), while potentially breaking mathematical structure by discarding crucial operator relationships. AvgPool [47], on the other hand, dilutes the semantic strength of key tokens and is insensitive to positional structure, failing to preserve the underlying formulation hierarchy. Although these methods have been widely adopted in other tasks, they demonstrate poor performance when applied to token selection in problem embeddings due to the unique structural and symbolic demands of mathematical optimization representations.

We propose a token selection method based on intra-sequence token similarity scores derived from the problem embedding, referred to as the ranked pool. Specifically, given a raw problem embedding sequence of length S , we define a similarity score matrix \mathbf{M}_{SI} , where each entry quantifies the similarity between a pair of token vectors. We compute pairwise similarities using PyTorch’s built-in `cosine_similarity()` function [47], where values approaching 1 indicate high similarity and those near 0 indicate low similarity. Formally, the similarity matrix is defined as

$$\mathbf{M}_{\text{SI}}[i][j] = \text{cosine_similarity}(\text{token}_i, \text{token}_j), \quad (5)$$

where token_i is the i -th token vector in the original sequence.

Next, we compute a similarity sum vector $\mathbf{V}_{\text{SUM_SI}}$, where each element $\mathbf{V}_{\text{SUM_SI}}[i]$ represents the total similarity score between token i and all other tokens

$$\mathbf{V}_{\text{SUM_SI}}[i] = \sum_{j \neq i} \mathbf{M}_{\text{SI}}[i][j]. \quad (6)$$

We then sort the tokens based on their $\mathbf{V}_{\text{SUM_SI}}$ values and select the m tokens with the lowest total similarity scores, corresponding to the most diverse tokens in the sequence. These m tokens are sequentially concatenated to form the pooled sequence. Here, m is a tunable hyperparameter chosen to be a small positive integer significantly smaller than the original sequence length.

Algorithm 1: Training of encoder-decoder.

Input: N training problems and their corresponding datasets $\mathcal{D} = \{\mathcal{D}_1, \dots, \mathcal{D}_i, \dots, \mathcal{D}_N\}$, the encoder model θ_E , the decoder model θ_D ;
Output: Trained models θ_E and θ_D ;

```

1 repeat
2   for zipped batch from  $\mathcal{D}$  do
3     for  $i = 1, \dots, N$  do
4        $\mathbf{x}, \mathbf{y} \leftarrow$  batch data from  $\mathcal{D}_i$ ;
5        $\mathbf{v}_{\text{joint}} \leftarrow \text{cat}(\mathbf{x}, \mathbf{y})$ ;
6        $\tilde{\mathbf{v}}_{\text{joint}} \leftarrow f_{\theta_D}(f_{\theta_E}(\mathbf{x}))$ ;
7        $\mathbf{v}_{\text{val}}, \mathbf{v}_{\text{type}} \leftarrow \text{split } \mathbf{v}_{\text{joint}}$ ;
8        $\tilde{\mathbf{v}}_{\text{val}}, \tilde{\mathbf{v}}_{\text{type}} \leftarrow \text{split } \tilde{\mathbf{v}}_{\text{joint}}$ ;
9        $\mathcal{L}_{\text{real}} \leftarrow \|\mathbf{v}_{\text{val}} - \tilde{\mathbf{v}}_{\text{val}}\|^2$ ;
10       $\mathcal{L}_{\text{class}} \leftarrow \text{CrossEntropyLoss}(\mathbf{v}_{\text{type}}, \tilde{\mathbf{v}}_{\text{type}})$ ;
11       $\mathcal{L} \leftarrow \mathcal{L}_{\text{real}} + \mathcal{L}_{\text{class}}$ ;
12      Backpropagation on  $\theta_E$  and  $\theta_D$  with  $\mathcal{L}$ ;
13    end
14  end
15 until convergence;
```

By selecting the most diverse tokens, the ranked pool effectively captures unique and informative symbolic elements, especially for those sensitive to small changes in mathematical expressions. Additionally, keeping the selected tokens in their original order helps preserve important structural relationships within the expression. In practice, ranked pool can be performed only once when the problem is first encountered, and the resulting pooled sequence can be cached for reuse, thereby avoiding repeated calls to the LLM for encoding and pooling. The experimental details are shown in Section V-B.

C. Problem-Aware Diffusion

We design a Transformer-based LDM [27] as the neural network component of PAD, with the Transformer [28] architecture as its backbone. Specifically, LDM is characterized by its ability to project variable-dimensional inputs from the data space into a fixed-dimensional latent space via an encoder, and then perform diffusion-based noise adding and denoising in this latent space. As illustrated in Fig. 2, our element-wise encoder maps each individual element in the input vector \mathbf{x} and solution vector \mathbf{y} into a token vector, in a way analogous to how a text encoder tokenizes characters. To account for the distinct physical meanings of different elements in \mathbf{x} and \mathbf{y} , we assign an integer label to each element representing its physical type (e.g., power, channel gain), allowing the encoder to generate discriminative embeddings. Let the encoder and decoder networks be parameterized by θ_E and θ_D , respectively. The training objective of the encoder-decoder is given as $f_{\theta_D}(f_{\theta_E}(\mathbf{x})) = \mathbf{x}$, where we apply mean squared error (MSE) loss on the element values and cross-entropy loss on the associated physical type labels. The training procedure is detailed in **Algorithm 1**.

For the backbone of PAD, we incorporate the ranked pool mechanism introduced in Section IV-B. As shown in Fig. 3, the encoded sequence of \mathbf{x} is concatenated with the pooled problem embedding sequence obtained via ranked pool, forming a condition sequence \mathbf{c} that guides the denoising process.

Algorithm 2: Training of constraint-aware module.

Input: N training problems and their corresponding datasets $\mathcal{D} = \{\mathcal{D}_1, \dots, \mathcal{D}_i, \dots, \mathcal{D}_N\}$ and problem embedding after ranked pooling $\{\mathbf{e}_1^p, \dots, \mathbf{e}_i^p, \dots, \mathbf{e}_N^p\}$, the constraint-aware module θ_C , constraint judgment tool function `if_satisfy_cons()`;
Output: Trained model θ_C ;

```

1 repeat
2   for zipped batch from  $\mathcal{D}$  do
3     for  $i = 1, \dots, N$  do
4        $\mathbf{x} \leftarrow$  batch data from  $\mathcal{D}_i$ ;
5        $\mathbf{y} \leftarrow$  randomly sampled solutions;
6        $\tilde{\mathbf{r}} \leftarrow f_{\theta_C}(\mathbf{e}_i^p, \mathbf{x}, \mathbf{y})$ ;
7        $\mathbf{r} \leftarrow \text{if\_satisfy\_cons}(\mathbf{e}_i^p, \mathbf{x}, \mathbf{y})$ ;
8        $\mathcal{L} \leftarrow \text{CrossEntropyLoss}(\mathbf{r}, \tilde{\mathbf{r}})$ ;
9       Backpropagation on  $\theta_C$  with  $\mathcal{L}$ ;
10    end
11  end
12 until convergence;
```

During training, the encoded optimal solution sequence \mathbf{z}_0 is progressively noised according to a diffusion schedule up to time step T , eventually yielding a pure Gaussian noise vector \mathbf{z}_T . The Transformer-based diffusion backbone θ_B takes the noisy vector \mathbf{z}_t and the condition sequence \mathbf{c} as input, and predicts the noise to be removed. The model is trained using MSE loss between the predicted and actual noise.

Here, \mathbf{c} and \mathbf{z}_t correspond to the source and target sequences for the Transformer, respectively. At inference time, we sample \mathbf{z}_T directly from Gaussian noise and iteratively apply θ_B to denoise it back to $\tilde{\mathbf{z}}_0$ without noise, which is then decoded to obtain the final generated solution $\tilde{\mathbf{y}}$.

D. Constraint-Aware Module

To improve the likelihood of generating feasible solutions, we design an independent constraint-aware module based on a TransformerEncoder [20] and a classification head. This module functions as a binary classifier that takes the input vector \mathbf{x} , the solution \mathbf{y} , and the pooled problem embedding as input, and predicts whether \mathbf{y} violates the hard constraints of the corresponding problem (outputting 1 if it does, and 0 otherwise). By approximating non-differentiable constraint functions through a differentiable neural network, this module introduces constraint violation penalties during the solution generation process, guiding the model toward producing valid solutions. This also increases the diversity and quality of feasible solutions discovered during parallel sampling. Augmenting the GDMs' noise prediction loss with additional preference-based objectives has proven effective in the AI community [48]. The training process of the constraint-aware module is detailed in **Algorithm 2**.

In implementation, we prepend a classification (CLS) token [49] to the input sequence and use its output representation for downstream classification. As provided in **Algorithm 3**, to mitigate the potential gradient interference between the noise prediction loss \mathcal{L}_{eps} and the constraint violation loss $\mathcal{L}_{\text{cons}}$, we apply $\mathcal{L}_{\text{cons}}$ only during the final phase of training. By introducing $\mathcal{L}_{\text{cons}}$ after \mathcal{L}_{eps} has largely converged, we enable more efficient optimization of $\mathcal{L}_{\text{cons}}$ while avoiding

Algorithm 3: Training of PAD backbone.

Input: N training problems and their corresponding datasets $\mathcal{D} = \{\mathcal{D}_1, \dots, \mathcal{D}_i, \dots, \mathcal{D}_N\}$ and problem embedding after ranked pooling $\{\mathbf{e}_1^p, \dots, \mathbf{e}_i^p, \dots, \mathbf{e}_N^p\}$, diffusion step T , constraint loss start epoch e , the trained models θ_C , θ_E and θ_D ;

Output: Trained model θ_B ;

```

1 repeat
2   for zipped batch from  $\mathcal{D}$  do
3     for  $i = 1, \dots, N$  do
4        $\mathbf{x}, \mathbf{y}^* \leftarrow$  batch data from  $\mathcal{D}_i$ ;
5        $\mathbf{c}_x, \mathbf{z}_0 \leftarrow f_{\theta_E}(\mathbf{x}, \mathbf{y}^*)$ ;
6        $\mathbf{c} \leftarrow \text{cat}(\mathbf{e}_i^p, \mathbf{c}_x)$ ;
7        $\mathbf{t} \leftarrow$  sample time step from Uniform(1,  $T$ );
8        $\epsilon \leftarrow$  sample noise from  $\mathcal{N}(0, \mathbf{I})$ ;
9        $\mathbf{z}_t \leftarrow$  noise adding on  $\mathbf{z}_0$  based on  $\epsilon$  and  $\mathbf{t}$ ;
10       $\tilde{\epsilon} \leftarrow f_{\theta_B}(\mathbf{c}, \mathbf{t}, \mathbf{z}_t)$ ;
11       $\mathcal{L}_{\text{eps}} \leftarrow \|\epsilon - \tilde{\epsilon}\|^2$ ;
12       $\mathcal{L}_{\text{cons}} \leftarrow 0$ ;
13      if in the last  $e$  epochs then
14         $\mathbf{z}_t, \tilde{\epsilon} \leftarrow$  select  $\mathbf{z}_t$  and the corresponding  $\tilde{\epsilon}$ 
15          where  $t < \frac{T}{2}$ ;
16         $\tilde{\mathbf{z}}_0 \leftarrow$  denoising on  $\mathbf{z}_t$  using  $\tilde{\epsilon}$ ;
17         $\mathcal{L}_{\text{cons}} \leftarrow f_{\theta_C}(\mathbf{e}_i^p, \mathbf{x}, f_{\theta_D}(\tilde{\mathbf{z}}_0))$ ;
18      end
19       $\mathcal{L} \leftarrow \mathcal{L}_{\text{eps}} + \mathcal{L}_{\text{cons}}$ ;
20      Backpropagation on  $\theta_B$  with  $\mathcal{L}$ ;
21    end
22  end
  
```

the convergence instability that may arise from joint training from the beginning. Moreover, we compute $\mathcal{L}_{\text{cons}}$ only for the final solutions derived from the denoising steps in the latter half of the diffusion process. This strategy ensures that the incorporation of constraints does not excessively disturb the denoising trajectory.

Once the encoder-decoder and constraint-aware module are trained, the overall training process of the PAD backbone is described in **Algorithm 3**, where all parameters outside the backbone are kept frozen.

V. EXPERIMENTS AND DISCUSSIONS

A. Experimental Settings

1) *Datasets:* We construct three variants (with 5, 6, and 7 optimization variables) for each of the six problems introduced in Section III-B. For each of these 18 problem settings, we produce a training set of 60,000 samples and a test set of 2,000 samples using the Gurobi solver [50]. All samples in the dataset are optimal solutions, and the detailed ranges of input parameters are provided in our open-source repository.

For clarity in presenting evaluation results, we refer to the six problems in Section III-B by short names: [“P1”, ..., “P6”]. Combined with their optimization dimensions, the test sets are named accordingly. For example, “P1_D5” denotes the test set for problem P1 with 5-dimensional optimization variables. We also assign each of the 18 problem settings a unique problem index ranging from 1 to 18. For instance, problem index 1 corresponds to “P1_D5”, and index 4 to “P2_D5”.

The original problem feature embeddings are generated using MathBERT [25], with each problem represented in LaTeX

mathematical format as input. The resulting embeddings typically range from 100 to 200 tokens in length, with each token having a dimensionality of 768. Although the token sequence lengths of DeepSeekMath [26] are comparable to those of MathBERT, the dimensionality per token reaches 4096 due to differences in its tokenizer or vocabulary. This leads to a prohibitively high computational cost in the token compression layer after pooling, and thus DeepSeekMath is omitted from subsequent experiments. Unless otherwise specified, we adopt our proposed ranked pool method with $m = 20$ for pooling the problem embeddings in the following experiments.

To analyze the model’s cross-problem generalization ability, we partition the six problems from Section III-B into training and testing subsets using two distinct strategies. Both partitioning strategies are based on inter-problem similarity scores derived from pooled problem embeddings, as described in Section V-B. Following the approach in Section IV-B, we compute the total similarity score of each problem with all others and sort them accordingly. In the first strategy, referred to as “ascending”, we select problems with the lowest total similarity scores for training. To ensure at least one unseen problem is left for evaluation, we construct five different training settings under this strategy. In the second strategy, referred to as “descending”, we instead select problems with the highest total similarity scores for training, resulting in five different training settings. Therefore, we explore 10 different training configurations for the backbone based on these two problem selection strategies.

All datasets were generated on a machine with two Intel(R) Xeon(R) Silver 4410Y processors. The problem was that embedding generation and model inference were both performed on an RTX 4090 24 GB.

2) *Model Settings:* For the encoder-decoder, we use a series of fully connected layers to embed the input parameter values into a `hidden_dim`-dimensional space, and an `nn.Embedding` layer to embed the parameter types into the latent space. During decoding, each token is decoded using several fully connected layers. The parameter values are predicted with a Sigmoid activation, while the parameter types are predicted with a Softmax activation. The encoder-decoder was trained following Algorithm 1 for 20 epochs with a batch size 256. The initial learning rate was set to 0.00015 and adjusted using a cosine annealing schedule.

For the PAD backbone, the Transformer is configured with a hidden dimension of 128, 8 attention heads, 6 encoder layers and 6 decoder layers. In the subsequent experiments, the PAD backbone is trained following Algorithm 3 for 50 epochs with a batch size of 2048. The diffusion setting adopts a Gaussian diffusion mechanism with 50 diffusion steps, cosine noise scheduling, DDIM [51] acceleration with 5 generation steps, and 2 parallel sampling runs during inference. In practice, many existing solution generation methods require tool-integrated reasoning or decoding strategies to further interpret the decoded solutions [22], [34], [52]. Our approach introduces a simple outside decoding step based on the absolute magnitude of each generated solution element prior to denormalization, without relying on any external reasoning tools.

For the constraint-aware module, it is implemented using

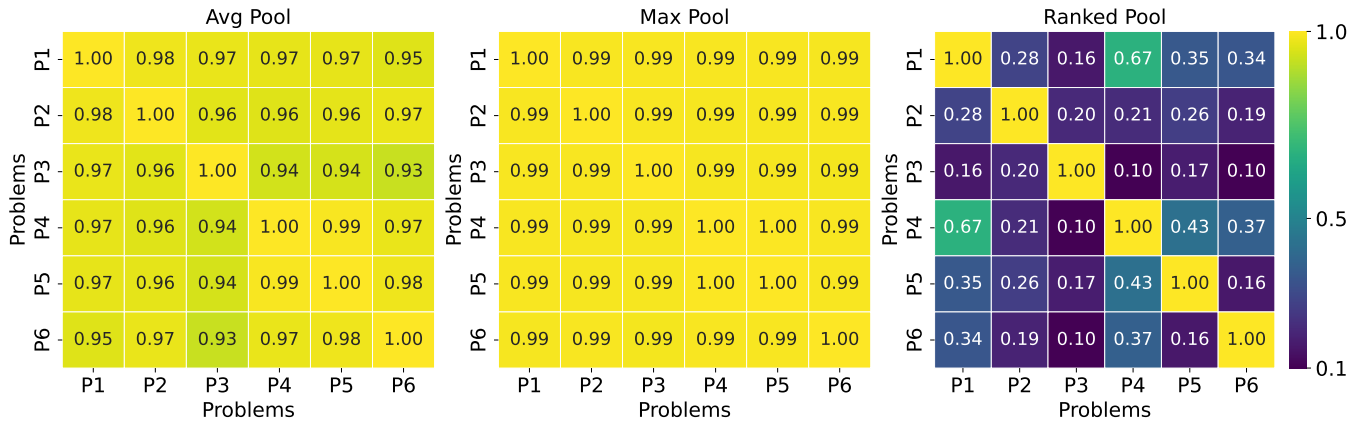


Fig. 4: The similarity score matrices between problems calculated on problem embeddings extracted using different pooling methods, where scores of two problems close to 1 represent high similarity and scores close to 0 represent low similarity.

only a TransformerEncoder architecture with the same parameter settings as the PAD backbone. In the experiments, it is trained according to Algorithm 2 for 10 epochs, with an additional 2-epoch fine-tuning applied to a few more complex problems. The batch size is set to 1024. Since uniformly sampled solutions for some problems may exhibit a strong imbalance between valid and invalid samples (e.g., over 80% of the training samples are labeled as violating constraints), which harms the model’s generalization ability. We apply oversampling during training to balance the distribution. Additionally, we assign different weights to the two classes in the CrossEntropyLoss, with a weight of 1.1 for label 0 and 1.0 for label 1. No oversampling is used during testing.

In training the backbone with the inclusion of constraint loss, two variables are considered: the method of computing the constraint loss and the epoch at which the constraint loss is introduced. We design two strategies for computing the constraint loss. The first, referred to as “default”, directly uses the output of the constraint-aware module as the loss value. The second, termed “t_increase”, applies a linear scaling to the module’s output based on the denoising timestep, assigning larger losses to noisy solutions closer to timestep 0. For each loss computation method, we explore five different epoch ratios for introducing the constraint loss: [0.2, 0.4, 0.6, 0.8, 1.0]. Each value denotes the proportion of the total training epochs during which the constraint loss is applied at the end of training. For example, the value 0.2 means that the constraint loss is applied only during the final 10 epochs of a 50-epoch training process. In total, this brings 10 distinct settings for constraint loss integration.

3) *Metrics*: To evaluate the quality of solutions generated by PAD, we define four metrics:

- **GT_GAP**: This metric directly measures solution quality by computing the absolute difference between 1 and the ratio of the generated solution’s objective value to the ground-truth optimal value, i.e., $GT_GAP = |\frac{f(x, \bar{y})}{f(x, y)} - 1|$. The final score is the average GT_GAP across all samples in the test set.
- **AVG_GT_GAP**: For more concise reporting, this simplified version of GT_GAP directly refers to the average

GT_GAP across all test problems.

- **CONS_ACC**: This evaluates constraint satisfaction across all generated solutions from parallel sampling. It is defined as the overall constraint satisfaction rate over all generated samples.
- **CONS_IF**: This metric evaluates whether at least one valid solution exists among the parallel samples for each input. A value of 1 is assigned if any valid solution exists, and 0 otherwise. The final score is the average over all test inputs.

To further analyze the performance of the constraint-aware module as a binary classifier, we use three standard metrics to assess its classification accuracy: global classification accuracy (ACC), true positive rate (TPR), recall for invalid solutions, and true negative rate (TNR), recall for valid solutions.

B. Analysis of Ranked Pool

1) *Specific Settings*: To empirically validate the effectiveness of the proposed ranked pool method for extracting fixed-length problem embeddings, we conduct a controlled comparison against two widely used pooling strategies: Max-Pool and AvgPool. All evaluations are performed under a consistent experimental setup trained on (P2,P3,P5,P6), with the constraint-aware module disabled to isolate the effects of the token pooling mechanism.

2) *Results*: In terms of solution quality, measured by the average GT_GAP across all test problems, the ranked pool shows consistent improvements over the baseline methods. Specifically, ranked pool yields an AVG_GT_GAP of 0.1263, compared to 0.1350 for MaxPool and 0.1370 for AvgPool. It suggests that the tokens selected via ranked pool better preserve the symbolic and structural nuances of the optimization problems, which are essential for accurate solution generation.

3) *Analysis of Problem Distinguishability*: To better understand the source of the observed performance differences, we analyze the ability of each pooling method to generate problem embeddings that distinguish between different optimization problems. We hypothesize that ranked pool promotes discriminative representations by preserving structural and symbolic distinctions across problems.

Comparison between with and without problem embedding on (GT_GAP ↓)

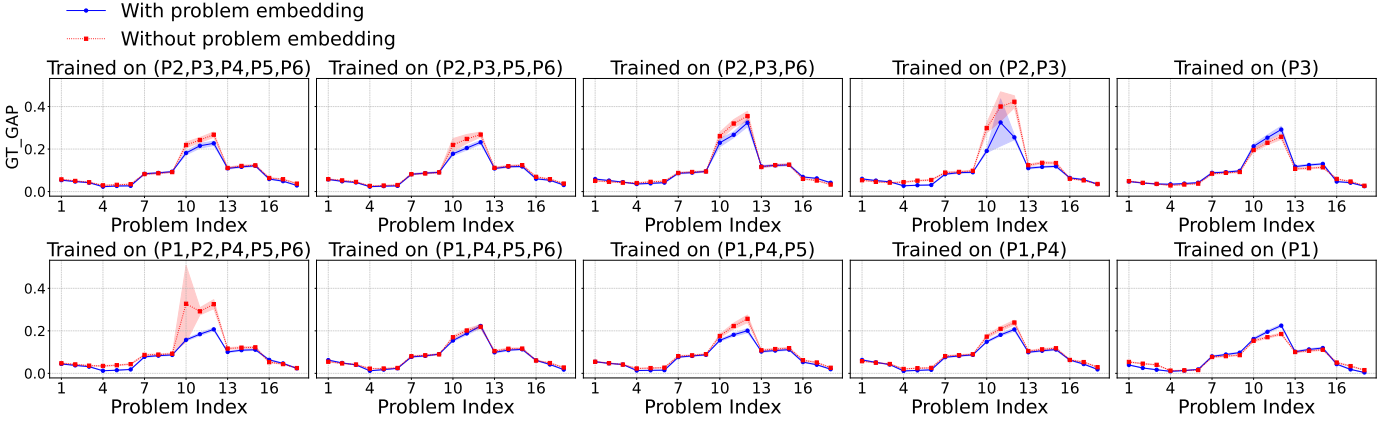


Fig. 5: Comparison on GT_GAP between models with and without problem feature embedding from 10 different training problem selections. Each line plot includes a light-colored shaded band representing the error bar given by the 95% confidence interval of the corresponding metric across all test samples. The line itself indicates the mean value. In the two rows of subplots, the training problem selection strategy for the first row is “ascending,” while for the second row it is “descending.” The specific training problems used for each subplot are indicated in the corresponding titles.

Comparison between with and without problem embedding on (CONS_ACC ↑)

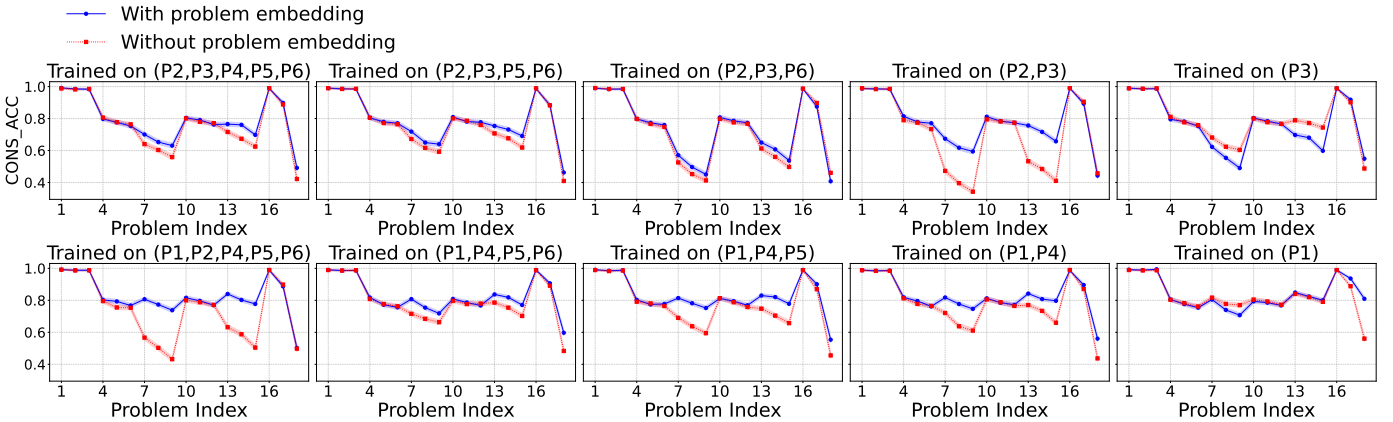


Fig. 6: Comparison on CONS_ACC between models with and without problem feature embedding from 10 different training problem selections. Each line plot includes a light-colored shaded band representing the error bar given by the 95% confidence interval of the corresponding metric across all test samples. The line itself indicates the mean value. In the two rows of subplots, the training problem selection strategy for the first row is “ascending,” while for the second row it is “descending.” The specific training problems used for each subplot are indicated in the corresponding titles.

To verify this, we compute pairwise cosine similarities between the pooled MathBERT embeddings of all 6 problems with different pool methods. For each pool method—AvgPool, MaxPool, and Ranked Pool—we apply the respective method to the original embeddings and calculate the resulting similarity matrix. The heatmaps are shown in Fig. 4.

The results reveal a clear pattern. MaxPool produces extremely high similarity scores (all above 0.98), indicating overly homogeneous embeddings that fail to differentiate between problems. AvgPool shows slightly more variation, but the similarities remain uniformly high, with most values above 0.90. In contrast, the ranked pool similarity matrix exhibits much greater variability: while semantically related problems (e.g., P1 and P4) retain moderately high similarity (above 0.5), unrelated problems show significantly lower scores, some as low as 0.1–0.3. This confirms that ranked pool can better

reflect symbolic and structural problem differences.

4) *Summary:* These findings support our hypothesis that token-level similarity analysis provides a more principled approach to selecting semantically rich and diverse tokens, especially in mathematical expressions where subtle symbolic differences matter. Unlike MaxPool, which may overemphasize frequent or high-activation tokens, and AvgPool, which tends to oversmooth, the ranked pool explicitly promotes token diversity and structural sensitivity through similarity-based ranking.

Overall, the ranked pool method offers a lightweight yet effective strategy for compressing long, symbolic representations into fixed-length embeddings. Its advantage lies not only in better capturing relevant token information but also in enhancing the distinguishability between problem instances for improving generalization in mathematical optimization tasks.

Comparison between after and before incorporating constraint loss on (GT_GAP↓)

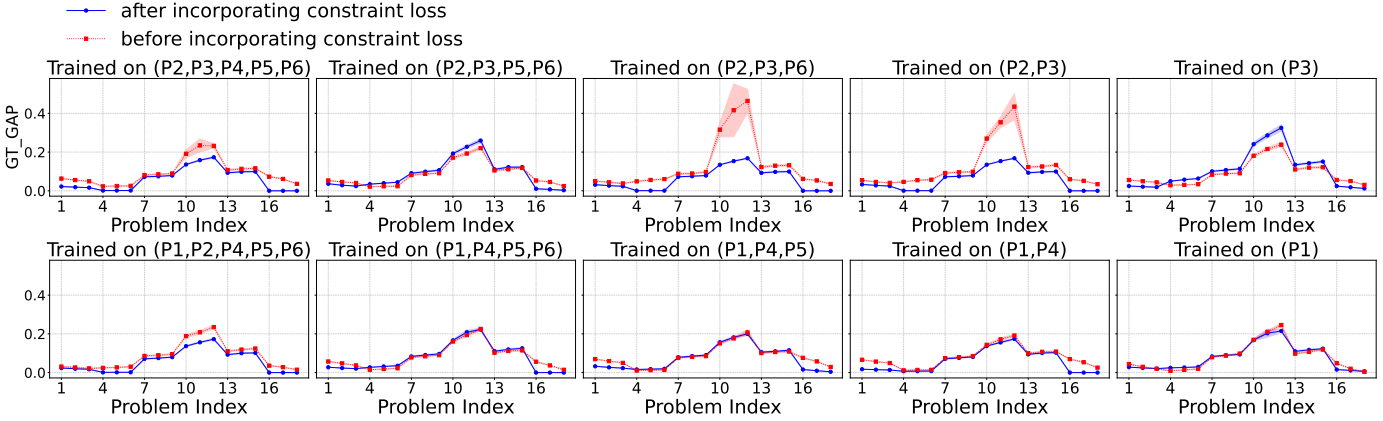


Fig. 7: Comparison on GT_GAP between models before and after incorporating constraint loss from 10 different training problem selections. Each line plot includes a light-colored shaded band representing the error bar given by the 95% confidence interval of the corresponding metric across all test samples. The line itself indicates the mean value. All subplots share a common y-axis scale. In the two rows of subplots, the training problem selection strategy for the first row is “ascending,” while for the second row it is “descending.” The specific training problems used for each subplot are indicated in the corresponding titles.

Comparison between after and before incorporating constraint loss on (CONS_ACC↑)

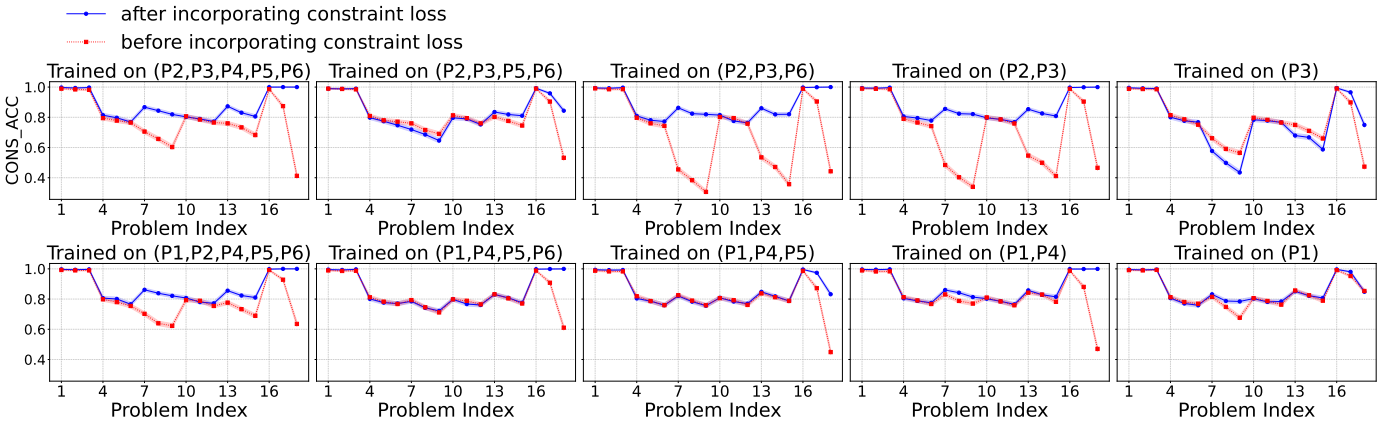


Fig. 8: Comparison on CONS_ACC between models before and after incorporating constraint loss from 10 different training problem selections. Each line plot includes a light-colored shaded band representing the error bar given by the 95% confidence interval of the corresponding metric across all test samples. The line itself indicates the mean value. In the two rows of subplots, the training problem selection strategy for the first row is “ascending,” while for the second row it is “descending.” The specific training problems used for each subplot are indicated in the corresponding titles.

C. Effectiveness of Problem Embedding

1) *Specific Settings:* To illustrate the effectiveness of incorporating problem feature embedding, we conduct experiments under the default training setup, exploring two variables: (1) whether problem feature embedding is included, and (2) the selection of the training problem set. This results in a total of 20 different experimental settings. We then evaluate the model using two metrics: GT_GAP and CONS_ACC.

2) *Results:* As shown in Fig. 5 and Fig. 6, models incorporating problem embedding (blue lines) generally outperform those without it (red lines), except in the extreme case where only a single problem is used for training. It can be observed that models without problem embedding exhibit higher variance on both metrics, particularly on GT_GAP. The model’s performance on unseen problems in the training set further

reflects its cross-problem generalization capability. For models without problem embedding, any degree of generalization is largely attributable to the benefits of parallel sampling and outside decoding. However, these models perform noticeably worse on CONS_ACC, since without problem embedding, the model lacks even the basic ability to identify the problem, let alone learn its characteristics.

The training problem selection for each subplot in Fig. 5 and Fig. 6 follows a specific strategy: the first row of subplots corresponds to the “ascending” strategy, while the second row corresponds to the “descending” strategy. Regarding the two problem selection strategies, the results show that “descending” consistently performs better. We believe the reason is that “descending” selects problems with the highest total similarity scores, effectively choosing the most representative and diverse problems from the problem space.

This also suggests that the higher the similarity between problems, the stronger the model’s potential for cross-problem generalization.

Regarding the number of training problems, it is naturally observed that more training problems lead to better overall performance. A few small exceptions exist—for instance, in Fig. 5, the two subplots “Trained on (P1,P4,P5,P6)” and “Trained on (P1,P4,P5)” show that for test problem index 12, the model trained on four problems slightly underperforms the one trained on three. This is mainly due to conflicting gradient directions among different problems during training; when more problems are jointly trained, performance trade-offs may arise. Although some multi-task learning techniques exist to mitigate such gradient conflicts, addressing this is beyond the scope of our current study.

Regarding problem characteristics, some of the six problems are inherently easier or more difficult. For instance, P1 is a constrained convex optimization problem, making it relatively simple, thus all models perform well on it. In contrast, P4 is a constrained integer programming problem, which is more complex. Combined with convergence issues caused by gradient conflicts across different problems, this leads to generally poor performance on P4 for all models.

As for cross-scale generalization, we observe a general trend where performance deteriorates as the problem dimension increases. This may be due to the data’s resource configuration. While the total amount of network resources remains nearly constant, the number of optimization variables increases, and the constraints remain unchanged. This significantly shrinks the feasible region and increases the problem’s complexity, impacting model performance.

3) *Summary*: Overall, the results in Fig. 5 and Fig. 6 demonstrate that incorporating problem feature embedding significantly enhances the model’s ability to generalize across different problems. This improvement is evident in both the quality and feasibility of the generated solutions, highlighting the strong potential of problem-aware learning.

D. Performance of Constraint-Aware Module

1) *Specific Settings*: To demonstrate the effectiveness of the constraint-aware module, we compare the PAD model’s performance before and after introducing the constraint loss. Through repeated experiments, we identify the best constraint loss configuration using the “default” loss computation method with an epoch introduction ratio of 0.6. We fix this configuration and conduct repeated experiments under 10 different training problem selection settings, comparing performance on the GT_GAP and CONS_ACC metrics. Additionally, we illustrate the constraint satisfaction classification performance of the shared frozen constraint-aware module using three metrics: ACC, TPR and TNR.

2) *Results*: As shown in Table I, the constraint-aware module achieves consistently high cross-problem classification accuracy (mostly above 0.95), particularly in identifying valid solutions, with TNR approaching 1 across the board. The classification accuracy is slightly lower for a few problems, such as P3, which only involves simple constraints like en-

TABLE I: The binary classification performance of the constraint-aware module.

	ACC↑	TPR↑	TNR↑
P1_D5	0.99	1.00	0.98
P1_D6	0.99	1.00	0.99
P1_D7	0.99	1.00	0.99
P2_D5	0.96	1.00	0.95
P2_D6	0.96	1.00	0.93
P2_D7	0.95	1.00	0.92
P3_D5	0.89	0.88	0.94
P3_D6	0.90	0.90	0.94
P3_D7	0.89	0.89	0.93
P4_D5	1.00	1.00	1.00
P4_D6	1.00	1.00	1.00
P4_D7	1.00	1.00	1.00
P5_D5	0.99	1.00	0.99
P5_D6	0.99	1.00	0.99
P5_D7	0.99	1.00	0.99
P6_D5	0.97	0.97	1.00
P6_D6	0.99	0.99	1.00
P6_D7	1.00	1.00	1.00

suring that allocated resources do not exceed the total available. We attribute this drop primarily to conflicting gradient directions during multi-problem training. Nevertheless, the overall accuracy of the constraint-aware module is sufficiently high for use in constraint loss computation, which effectively penalizes invalid solutions and rarely misclassifies valid ones. After introducing the constraint loss, CONS_IF improved from mostly above 0.8—with some cases as low as 0.64—to consistently above 0.92. With a slight increase in the number of parallel samples (e.g., to 4), it can approach 1.

As shown in Fig. 7 and Fig. 8, models incorporating the constraint loss (blue lines) generally perform better, particularly in terms of CONS_ACC, where improvements of up to 60% are observed for certain problems. The increase in CONS_ACC allows the parallel sampling process to cover a broader space of valid solutions, making it easier to reach better overall solutions and thus directly improving GT_GAP as well.

In some cases, the improvement in CONS_ACC plateaus after introducing the constraint loss. We believe this is due to the upper performance bound imposed by joint training across multiple problems. Additionally, in certain cases, the change in CONS_ACC is minimal while GT_GAP improves significantly, such as P4 in the “Trained on (P2, P3)” subplots. This suggests that the constraint-aware module’s implicit understanding of problem-specific constraints may also contribute to the quality of the generated feasible solutions.

3) *Summary*: In summary, the results presented in Fig. 7 and Fig. 8 demonstrate that incorporating constraint loss significantly improves the feasibility of the solutions generated by the PAD model, while also contributing to better overall solution quality. These findings validate the effectiveness of the constraint-aware module and highlight the potential of using constraint loss to enhance the feasibility of model outputs.

VI. CONCLUSION AND FUTURE DIRECTIONS

This paper has demonstrated a problem-aware learning approach for cross-problem network optimization, aiming to

provide general-purpose solution capabilities for fundamental models in wireless communication networks. Specifically, we have designed a problem-aware diffusion (PAD) model that explicitly incorporates the mathematical representations of problem formulations via problem embedding. This enables the model to recognize and understand the mathematical structure of optimization problems.

We have identified three key insights from experiments on six representative network optimization problems, which vary in type and complexity. First, the mathematical formulations of network optimization problems contain rich structural and semantic information. Even simple compressed representations can serve as effective and logically consistent problem feature embeddings. Second, explicitly introducing these embeddings during model training and inference significantly enhances cross-problem generalization, allowing the model to generate high-quality solutions even for previously unseen problems. Third, constructing an auxiliary constraint-aware module for identifying infeasible solutions and applying it as a loss function can effectively improve the feasibility of generated solutions, while also contributing positively to solution quality. These insights offer a foundational direction for building general-purpose AI models for wireless networks, especially in tasks such as network operation and resource management.

Additionally, several aspects of the current work warrant further investigation. From an engineering perspective, multi-task learning, model compression, and real-world deployment of the PAD model remain essential considerations. On a deeper level, the current PAD framework does not yet incorporate mathematical analysis of different optimization problem characteristics, nor does it learn corresponding mathematical reasoning strategies. We believe that new neural architecture designs and optimization-specific learning objectives are necessary to further enhance the effectiveness of problem-aware learning.

REFERENCES

- [1] K. B. Letaief, W. Chen, Y. Shi, J. Zhang, and Y.-J. A. Zhang, "The Roadmap to 6G: AI Empowered Wireless Networks," *IEEE Communications Magazine*, vol. 57, no. 8, pp. 84–90, 2019.
- [2] H. Zou, Q. Zhao, L. Bariah, M. Bennis, and M. Debbah, "Wireless Multi-Agent Generative AI: From Connected Intelligence to Collective Intelligence," 2023. [Online]. Available: <https://arxiv.org/abs/2307.02757>
- [3] X. Cao, B. Yang, K. Wang, X. Li, Z. Yu, C. Yuen, Y. Zhang, and Z. Han, "AI-Empowered Multiple Access for 6G: A Survey of Spectrum Sensing, Protocol Designs, and Optimizations," *Proceedings of the IEEE*, vol. 112, no. 9, pp. 1264–1302, 2024.
- [4] F. Ayed, A. Maatouk, N. Piovesan, A. D. Domenico, M. Debbah, and Z.-Q. Luo, "Hermes: A Large Language Model Framework on the Journey to Autonomous Networks," 2024. [Online]. Available: <https://arxiv.org/abs/2411.06490>
- [5] Z. Li, Q. Wang, Y. Wang, and T. Chen, "The Architecture of AI and Communication Integration towards 6G: An O-RAN Evolution," in *Proceedings of the 30th Annual International Conference on Mobile Computing and Networking*. Association for Computing Machinery, 2024, p. 2329–2334.
- [6] R. Liang, B. Yang, P. Chen, X. Cao, Z. Yu, M. Debbah, D. Niyato, H. V. Poor, and C. Yuen, "GDGS: Graph Diffusion-based Solution Generator for Optimization Problems in MEC Networks," 2024. [Online]. Available: <https://arxiv.org/abs/2412.08296>
- [7] M. Kotaru, "Adapting Foundation Models for Operator Data Analytics," in *Proceedings of the 22nd ACM Workshop on Hot Topics in Networks*. Association for Computing Machinery, 2023, p. 172–179.
- [8] G. Berardinelli and R. Adeogun, "Hybrid Radio Resource Management for 6G Subnetwork Crowds," *IEEE Communications Magazine*, vol. 61, no. 6, pp. 148–154, 2023.
- [9] T. Mongaillard, S. Lasaulce, O. Hicheur, C. Zhang, L. Bariah, V. S. Varma, H. Zou, Q. Zhao, and M. Debbah, "Large Language Models for Power Scheduling: A User-Centric Approach," in *Proceedings of 22nd International Symposium on Modeling and Optimization in Mobile, Ad Hoc, and Wireless Networks (WiOpt)*, 2024, pp. 321–328.
- [10] S. Waskito, K. J. Leow, P. Medaranga, T. Gupta, S. Chakrabarty, M. Gulati, and A. Varshney, "Otter: Simplifying Embedded Sensor Data Collection and Analysis using Large Language Models," in *Proceedings of the 29th Annual International Conference on Mobile Computing and Networking*. Association for Computing Machinery, 2023.
- [11] Y. Shi, L. Lian, Y. Shi, Z. Wang, Y. Zhou, L. Fu, L. Bai, J. Zhang, and W. Zhang, "Machine Learning for Large-Scale Optimization in 6G Wireless Networks," *IEEE Communications Surveys & Tutorials*, vol. 25, no. 4, pp. 2088–2132, 2023.
- [12] L. Luo, G. Zhao, H. Xu, Z. Yu, and L. Xie, "TanGo: A Cost Optimization Framework for Tenant Task Placement in Geo-distributed Clouds," in *Proceedings of IEEE Conference on Computer Communications*, 2023, pp. 1–10.
- [13] J. Zhang and D. M. Blough, "Optimizing Coverage with Intelligent Surfaces for Indoor mmWave Networks," in *Proceedings of IEEE Conference on Computer Communications*, 2022, pp. 830–839.
- [14] H. Zhang, X. Ma, X. Liu, L. Li, and K. Sun, "GNN-Based Power Allocation and User Association in Digital Twin Network for the Terahertz Band," *IEEE Journal on Selected Areas in Communications*, vol. 41, no. 10, pp. 3111–3121, 2023.
- [15] Y. Zhao, C. H. Liu, T. Yi, G. Li, and D. Wu, "Energy-Efficient Ground-Air-Space Vehicular Crowdsensing by Hierarchical Multi-Agent Deep Reinforcement Learning With Diffusion Models," *IEEE Journal on Selected Areas in Communications*, vol. 42, no. 12, pp. 3566–3580, 2024.
- [16] Y. Zhong, J. Kang, J. Wen, D. Ye, J. Nie, D. Niyato, X. Gao, and S. Xie, "Generative Diffusion-Based Contract Design for Efficient AI Twin Migration in Vehicular Embodied AI Networks," *IEEE Transactions on Mobile Computing*, pp. 1–16, 2025.
- [17] S. Fujimoto, P. D'Oro, A. Zhang, Y. Tian, and M. Rabbat, "Towards General-Purpose Model-Free Reinforcement Learning," in *Proceedings of The Thirteenth International Conference on Learning Representations*, 2025. [Online]. Available: <https://arxiv.org/abs/2501.16142>
- [18] H. Du, Z. Li, D. Niyato, J. Kang, Z. Xiong, H. Huang, and S. Mao, "Diffusion-Based Reinforcement Learning for Edge-Enabled AI-Generated Content Services," *IEEE Transactions on Mobile Computing*, vol. 23, no. 9, pp. 8902–8918, 2024.
- [19] T. Ren, Z. Hu, H. He, J. Niu, and X. Liu, "FEAT: Towards Fast Environment-Adaptive Task Offloading and Power Allocation in MEC," in *Proceedings of IEEE Conference on Computer Communications*, 2023, pp. 1–10.
- [20] H. Du, J. Wang, D. Niyato, J. Kang, Z. Xiong, and D. I. Kim, "AI-Generated Incentive Mechanism and Full-Duplex Semantic Communications for Information Sharing," *IEEE Journal on Selected Areas in Communications*, vol. 41, no. 9, pp. 2981–2997, 2023.
- [21] N. Kan, S. Yan, J. Zou, W. Dai, X. Gao, C. Li, and H. Xiong, "GDPlan: Generative Network Planning via Graph Diffusion Model," *IEEE Transactions on Networking*, pp. 1–16, 2025.
- [22] K. Yang, G. Poesia, J. He, W. Li, K. Lauter, S. Chaudhuri, and D. Song, "Formal Mathematical Reasoning: A New Frontier in AI," 2024. [Online]. Available: <https://arxiv.org/abs/2412.16075>
- [23] I. Drori, S. Zhang, R. Shuttleworth, L. Tang, A. Lu, E. Ke, K. Liu, L. Chen, S. Tran, N. Cheng, R. Wang, N. Singh, T. L. Patti, J. Lynch, A. Shporer, N. Verma, E. Wu, and G. Strang, "A neural network solves, explains, and generates university math problems by program synthesis and few-shot learning at human level," *Proceedings of the National Academy of Sciences*, vol. 119, no. 32, p. e2123433119, 2022.
- [24] H. Zou, Q. Zhao, Y. Tian, L. Bariah, F. Bader, T. Lestable, and M. Debbah, "TelecomGPT: A Framework to Build Telecom-Specific Large Language Models," 2024. [Online]. Available: <https://arxiv.org/abs/2407.09424>
- [25] S. Peng, K. Yuan, L. Gao, and Z. Tang, "MathBERT: A Pre-Trained Model for Mathematical Formula Understanding," 2021. [Online]. Available: <https://arxiv.org/abs/2105.00377>
- [26] Z. Shao, P. Wang, Q. Zhu, R. Xu, J. Song, X. Bi, H. Zhang, M. Zhang, Y. K. Li, Y. Wu, and D. Guo, "DeepSeekMath: Pushing the Limits of Mathematical Reasoning in Open Language Models," 2024. [Online]. Available: <https://arxiv.org/abs/2402.03300>

[27] R. Rombach, A. Blattmann, D. Lorenz, P. Esser, and B. Ommer, "High-Resolution Image Synthesis With Latent Diffusion Models," in *Proceedings of the IEEE/CVF Conference on Computer Vision and Pattern Recognition (CVPR)*, June 2022, pp. 10 684–10 695.

[28] A. Vaswani, N. Shazeer, N. Parmar, J. Uszkoreit, L. Jones, A. N. Gomez, L. Kaiser, and I. Polosukhin, "Attention is all you need," in *Proceedings of the 31st International Conference on Neural Information Processing Systems*. Curran Associates Inc., 2017, p. 6000–6010.

[29] D. Wu, X. Wang, Y. Qiao, Z. Wang, J. Jiang, S. Cui, and F. Wang, "NetLLM: Adapting Large Language Models for Networking," in *Proceedings of the ACM SIGCOMM Conference*. Association for Computing Machinery, 2024, p. 661–678.

[30] H. Li, M. Xiao, K. Wang, D. I. Kim, and M. Debbah, "Large Language Model Based Multi-Objective Optimization for Integrated Sensing and Communications in UAV Networks," *IEEE Wireless Communications Letters*, pp. 1–1, 2025.

[31] J. Wang, H. Du, Y. Liu, G. Sun, D. Niyato, S. Mao, D. I. Kim, and X. Shen, "Generative ai based secure wireless sensing for isac networks," 2024. [Online]. Available: <https://arxiv.org/abs/2408.11398>

[32] R. Liang, B. Yang, Z. Yu, B. Guo, X. Cao, M. Debbah, H. V. Poor, and C. Yuen, "DiffSG: A Generative Solver for Network Optimization with Diffusion Model," 2025. [Online]. Available: <https://arxiv.org/abs/2408.06701>

[33] R. Liang, B. Yang, P. Chen, X. Li, Y. Xue, Z. Yu, X. Cao, Y. Zhang, M. Debbah, H. V. Poor, and C. Yuen, "Diffusion Models as Network Optimizers: Explorations and Analysis," *IEEE Internet of Things Journal*, pp. 1–1, 2025.

[34] Y. Li, J. Liu, Q. Wu, X. Qin, and J. Yan, "Toward Learning Generalized Cross-Problem Solving Strategies for Combinatorial Optimization," 2025. [Online]. Available: <https://openreview.net/forum?id=VnaJNW8OpN>

[35] H. Lei, K. Zhou, Y. Li, Z. Chen, and F. Farnia, "Boosting Generalization in Diffusion-Based Neural Combinatorial Solver via Energy-guided Sampling," 2025. [Online]. Available: <https://arxiv.org/abs/2502.12188>

[36] M. Krichen, A. Mihoub, M. Y. Alzahrani, W. Y. H. Adoni, and T. Nahhal, "Are Formal Methods Applicable To Machine Learning And Artificial Intelligence?" in *Proceedings of 2nd International Conference of Smart Systems and Emerging Technologies (SMARTTECH)*, 2022, pp. 48–53.

[37] C. Yang, X. Wang, Y. Lu, H. Liu, Q. V. Le, D. Zhou, and X. Chen, "Large Language Models as Optimizers," 2024. [Online]. Available: <https://arxiv.org/abs/2309.03409>

[38] F. Gong, D. Raghunathan, A. Gupta, and M. Apostolaki, "Towards Integrating Formal Methods into ML-Based Systems for Networking," in *Proceedings of the 22nd ACM Workshop on Hot Topics in Networks*. Association for Computing Machinery, 2023, p. 48–55.

[39] H. He, C. Bai, K. Xu, Z. Yang, W. Zhang, D. Wang, B. Zhao, and X. Li, "Diffusion Model is an Effective Planner and Data Synthesizer for Multi-Task Reinforcement Learning," in *Proceedings of Advances in Neural Information Processing Systems*, vol. 36. Curran Associates, Inc., 2023, pp. 64 896–64 917.

[40] C. Fan, C. Bai, Z. Shan, H. He, Y. Zhang, and Z. Wang, "Task-agnostic Pre-training and Task-guided Fine-tuning for Versatile Diffusion Planner," 2025. [Online]. Available: <https://arxiv.org/abs/2409.19949>

[41] C. Zhan, H. Hu, S. Mao, and J. Wang, "Energy-Efficient Trajectory Optimization for Aerial Video Surveillance under QoS Constraints," in *Proceedings of IEEE Conference on Computer Communications*, 2022, pp. 1559–1568.

[42] A. Coletta, F. Giorgi, G. Maselli, M. Prata, D. Silvestri, J. Ashdown, and F. Restuccia, "A2-UAV: Application-Aware Content and Network Optimization of Edge-Assisted UAV Systems," in *Proceedings of IEEE Conference on Computer Communications*, 2023, pp. 1–10.

[43] L. Liang, H. Ye, and G. Y. Li, "Spectrum Sharing in Vehicular Networks Based on Multi-Agent Reinforcement Learning," *IEEE Journal on Selected Areas in Communications*, vol. 37, no. 10, pp. 2282–2292, 2019.

[44] A. C. Cullen, B. I. Rubinstein, S. Kandeepan, B. Flower, and P. H. Leong, "Predicting dynamic spectrum allocation: a review covering simulation, modelling, and prediction," *Artificial Intelligence Review*, vol. 56, no. 10, pp. 10 921–10 959, 2023.

[45] Y. Mao, C. You, J. Zhang, K. Huang, and K. B. Letaief, "A Survey on Mobile Edge Computing: The Communication Perspective," *IEEE Communications Surveys & Tutorials*, vol. 19, no. 4, pp. 2322–2358, 2017.

[46] Q. Duan, J. Huang, S. Hu, R. Deng, Z. Lu, and S. Yu, "Combining Federated Learning and Edge Computing Toward Ubiquitous Intelligence in 6G Network: Challenges, Recent Advances, and Future Directions,"

IEEE Communications Surveys & Tutorials, vol. 25, no. 4, pp. 2892–2950, 2023.

[47] A. Paszke, S. Gross, F. Massa, A. Lerer, J. Bradbury, G. Chanan, T. Killeen, Z. Lin, N. Gimelshein, L. Antiga, A. Desmaison, A. Köpf, E. Yang, Z. DeVito, M. Raison, A. Tejani, S. Chilamkurthy, B. Steiner, L. Fang, J. Bai, and S. Chintala, *PyTorch: an imperative style, high-performance deep learning library*. Curran Associates Inc., 2019.

[48] A. Radford, J. W. Kim, C. Hallacy, A. Ramesh, G. Goh, S. Agarwal, G. Sastry, A. Askell, P. Mishkin, J. Clark, G. Krueger, and I. Sutskever, "Learning Transferable Visual Models From Natural Language Supervision," in *Proceedings of International Conference on Machine Learning*, 2021.

[49] J. Devlin, M.-W. Chang, K. Lee, and K. Toutanova, "BERT: Pre-training of Deep Bidirectional Transformers for Language Understanding," in *Proceedings of North American Chapter of the Association for Computational Linguistics*, 2019.

[50] Gurobi Optimization, LLC, "Gurobi Optimizer Reference Manual," 2024. [Online]. Available: <https://www.gurobi.com>

[51] J. Song, C. Meng, and S. Ermon, "Denosing Diffusion Implicit Models," 2022. [Online]. Available: <https://arxiv.org/abs/2010.02502>

[52] Z. Sun and Y. Yang, "DIFUSCO: Graph-based Diffusion Solvers for Combinatorial Optimization," in *Proceedings of Advances in Neural Information Processing Systems*, A. Oh, T. Naumann, A. Globerson, K. Saenko, M. Hardt, and S. Levine, Eds., vol. 36. Curran Associates, Inc., 2023, pp. 3706–3731.

APPENDIX

MODELING OF THE SELECTED PROBLEMS

We now present the detailed mathematical formulations and settings for the six selected network optimization problems introduced in Section III-B. The variable symbols used in each problem are isolated from those in other problems, with no reuse across problems.

- 1) **P1** aims to maximize the total transmission rate under constraints on total power and per-channel minimum rate requirements. Specifically, M denotes the number of channels, B [Hz] represents the default bandwidth of each OFDMA [3] channel, and P_{total} [W] denotes the total available power. The sets $\{g_1, \dots, g_M\}$ and $\{N_1, \dots, N_M\}$ represent the channel gains and noise power spectral density for each channel, respectively. Variable: Continuous power allocation $\{p_1, \dots, p_M\}$ [W] for each channels $m = \{1, \dots, M\}$.

Objective:

$$\max_{\{p_1, \dots, p_M\}} \sum_{m=1}^M B \log_2 \left(1 + \frac{g_m p_m}{B N_m} \right)$$

Constraints:

$$\sum_{m=1}^M p_m \leq P_{\text{total}},$$

$$B \log_2 \left(1 + \frac{g_m p_m}{B N_m} \right) \geq R_{\text{min}},$$

$$p_m \geq 0, \forall m \in \{1, \dots, M\}$$

This modeling belongs to a classic category of wireless resource allocation problems [9], [12], [14].

- 2) **P2** aims to maximize the power efficiency, defined as the ratio of transmission rate to consumed power, under constraints on total power and minimum rate requirements for each channel. Specifically, M denotes the number of channels, B [Hz] represents the default bandwidth of each OFDMA [3] channel, and P_{total} [W] denotes the total available power. The sets $\{g_1, \dots, g_M\}$ and $\{N_1, \dots, N_M\}$ represent the channel gains and noise power spectral density for each channel, respectively. Variable: Continuous power allocation $\{p_1, \dots, p_M\}$ for each channels $m = \{1, \dots, M\}$.

Objective:

$$\max_{\{p_1, \dots, p_M\}} \sum_{m=1}^M \frac{B \log_2 \left(1 + \frac{g_m p_m}{B N_m} \right)}{p_m}$$

Constraints:

$$\begin{aligned} \sum_{m=1}^M p_m &\leq P_{\text{total}}, \\ B \log_2 \left(1 + \frac{g_m p_m}{B N_m} \right) &\geq R_{\min}, \\ p_m &\geq 0, \forall m \in \{1, \dots, M\} \end{aligned}$$

Maximizing power efficiency is particularly relevant in scenarios where power savings are required based on channel quality conditions [9], [12], [14].

- 3) **P3** aims to minimize the maximum transmission delay across all channels, defined as the ratio between the data volume and the corresponding achievable transmission rate, under a constraint on the total transmit power. Specifically, M denotes the number of channels, B [Hz] represents the default bandwidth of each OFDMA [3] channel, and P_{total} [W] denotes the total available power. And $\{d_1, \dots, d_M\}$ [bit] denotes the amount of data that needs to be transmitted for each connection. The sets $\{g_1, \dots, g_M\}$ and $\{N_1, \dots, N_M\}$ represent the channel gains and noise power spectral density for each channel, respectively. Variable: Continuous power allocation $\{p_1, \dots, p_M\}$ for each channels $m = \{1, \dots, M\}$.

Objective:

$$\min_{\{p_1, \dots, p_M\}} \max_m \frac{d_m}{B \log_2 \left(1 + \frac{g_m p_m}{B N_m} \right)}$$

Constraints:

$$\begin{aligned} \sum_{m=1}^M p_m &\leq P_{\text{total}}, \\ p_m &\geq 0, \forall m \in \{1, \dots, M\} \end{aligned}$$

This type of problem represents a fundamental class of transmission tasks [15]. At the same time, as a maximization-oriented optimization problem, it also contributes to the diversity of our problem set.

- 4) **P4** aims to maximize the total transmission rate, under constraints on the total available spectrum resource block and minimum rate requirements for each channel. Specifically, M denotes the number of channels. Since in real-world scenarios, spectrum resources are typically allocated in discrete blocks rather than continuous values, we define B_{total} as the total number of resource blocks and b [Hz] as the bandwidth of each block. The sets $\{g_1, \dots, g_M\}$ and $\{N_1, \dots, N_M\}$ represent the channel gains and noise power spectral density for each channel, respectively. The $\{p_1, \dots, p_M\}$ represent the transmission powers for each channel.

Variable: Discrete spectrum resource block allocation $\{B_1, \dots, B_M\}$ for each channel $m = \{1, \dots, M\}$.

Objective:

$$\max_{\{B_1, \dots, B_M\}} \sum_{m=1}^M B_m b \log_2 \left(1 + \frac{g_m p_m}{B_m b N_m} \right)$$

Constraints:

$$\begin{aligned} \sum_{m=1}^M B_m &\leq B_{\text{total}}, \\ B_m b \log_2 \left(1 + \frac{g_m p_m}{B_m b N_m} \right) &\geq R_{\min}, \\ B_m &\geq 0, \forall m \in \{1, \dots, M\} \end{aligned}$$

This represents another classic category of wireless resource allocation problems [3], [8], [43], where the inclusion of discrete optimization variables further enhances the realism of our problem set.

- 5) **P5** aims to maximize the overall spectral efficiency, defined as the ratio of achievable rate to allocated bandwidth, under

constraints on total spectrum and minimum per-channel rate requirements. Specifically, M denotes the number of channels. Given B_{total} as the total number of resource blocks and b [Hz] as the bandwidth of each block. The sets $\{g_1, \dots, g_M\}$ and $\{N_1, \dots, N_M\}$ represent the channel gains and noise power spectral density for each channel, respectively. The $\{p_1, \dots, p_M\}$ represent the transmission powers for each channel.

Variable: Discrete spectrum resource block allocation $\{B_1, \dots, B_M\}$ for each channel $m = \{1, \dots, M\}$.

Objective:

$$\max_{\{B_1, \dots, B_M\}} \sum_{m=1}^M \frac{\log_2 \left(1 + \frac{g_m p_m}{B_m b N_m} \right)}{B_m}$$

Constraints:

$$\begin{aligned} \sum_{m=1}^M B_m &\leq B_{\text{total}}, \\ B_m b \log_2 \left(1 + \frac{g_m p_m}{B_m b N_m} \right) &\geq R_{\min}, \\ B_m &\geq 0, \forall m \in \{1, \dots, M\} \end{aligned}$$

Similarly, maximizing spectral efficiency is relevant in scenarios where spectrum conservation is needed based on channel quality and terminal device power conditions [3], [8], [43].

- 6) **P6** aims to maximize the total transmission rate under constraints on total spectrum availability and fairness across channels based on predefined weights. Specifically, M denotes the number of channels. Given B_{total} as the total number of resource blocks and b [Hz] as the bandwidth of each block. The sets $\{g_1, \dots, g_M\}$ and $\{N_1, \dots, N_M\}$ represent the channel gains and noise power spectral density for each channel, respectively. The $\{p_1, \dots, p_M\}$ represent the transmission powers for each channel. Additionally, $\{\alpha_1, \dots, \alpha_M\}$ denotes the contribution factors associated with each connected terminal device, while θ represents the minimum transmission rate required by the system under a specified contribution ratio.

Variable: Discrete spectrum resource block allocation $\{B_1, \dots, B_M\}$ for each channel $m = \{1, \dots, M\}$.

Objective:

$$\max_{\{B_1, \dots, B_M\}} \sum_{m=1}^M B_m b \log_2 \left(1 + \frac{g_m p_m}{B_m b N_m} \right)$$

Constraints:

$$\begin{aligned} \sum_{m=1}^M B_m &\leq B_{\text{total}}, \\ \frac{B_m b \log_2 \left(1 + \frac{g_m p_m}{B_m b N_m} \right)}{\alpha_m} &\geq \theta, \\ B_m &\geq 0, \forall m \in \{1, \dots, M\} \end{aligned}$$

The problem's constraint imposes different minimum rate requirements for each connection, which can be generalized to distributed weight synchronization tasks in typical federated learning settings [46].

The selection of the above problems ensures that our problem set encompasses a diverse and realistic range of resource types, optimization variables, objectives, and constraints.